PVP-Vol. 104

Flow-Induced Vibration — 1986

edited by
S. S. CHEN
J. C. SIMONIS
Y. S. SHIN

PVP-Vol. 104

Flow-Induced Vibration — 1986

presented at

THE 1986 PRESSURE VESSELS AND PIPING
CONFERENCE AND EXHIBITION
CHICAGO, ILLINOIS
JULY 20–24, 1986

sponsored by

OPERATIONS, APPLICATIONS, AND COMPONENTS COMMITTEE,
THE PRESSURE VESSEL AND PIPING DIVISION, ASME

edited by

S. S. CHEN
ARGONNE NATIONAL LABORATORY
ARGONNE, ILLINOIS

J. C. SIMONIS
SOUTHWEST RESEARCH INSTITUTE
SAN ANTONIO, TEXAS

Y. S. SHIN
NAVAL POSTGRADUATE SCHOOL
MONTEREY, CALIFORNIA

THE AMERICAN SOCIETY OF MECHANICAL ENGINEERS
United Engineering Center 345 East 47th Street New York, N.Y. 10017

Library of Congress Catalog Card Number 86-71376

FOREWORD

Flow induced vibration is a subject of current interest and has received continuing attention. It also has been the topic of a series of symposia sponsored by the Operations, Applications, and Components Committee. The objective of this symposium is to provide a forum for the exchange of information and to contribute to the state-of-the-art of flow induced vibration. The editors are particularly pleased that a number of authors have presented their practical experience—both successful and unsuccessful—and the symposium is truly an international one, with authors representing nine countries.

Twenty-five papers are presented covering axial flow, crossflow, acoustic resonance, fluid damping, and fluid/structure interaction. Components discussed include heat exchanger tube bundles, transmission lines, thermal shields, Space Shuttle Main Engines, pipes, and other system components. Papers presented include fundamental studies of basic mechanisms, experimental data on structural response and fluid forces, development of analysis techniques, comparison of theoretical and experimental results, and assessment of practical system components. The papers cover a wide range of problems that are representative of current research.

The papers contained in this volume can be divided into four groups:

- Fluid Excitation Forces: The fluid forces experienced by tube arrays in crossflow depend on tube arrangement, Reynolds number, upstream flow field, and tube location. Four papers present the flow field and fluid excitation forces for two tubes and tube arrays in single or two-phase flow; the data include Strouhal number, pressure fluctuation, drag and lift forces, and power spectral density of fluid force and flow velocity.
- Axial Flow Induced Vibration: Shells and pipes are the main concern in this group of papers. Topics include dynamic instability of Weir in an advanced reactor, pipes conveying fluid, and degradation of a thermal shield design.
- Fluid Damping: When a structural component vibrates in a fluid, the resultant fluid effect can be accounted for using added mass, fluid damping, and fluid stiffness. Four papers are directed to the analysis and measurements of fluid damping in quiescent fluid.
- Crossflow Induced Vibration of Multiple Cylinders: About half the papers are on this subject, which reflects the significance of this problem. The components considered vary from condenser tube to the liquid oxygen posts. The mechanisms discussed cover fluidelastic instability, turbulent buffeting, vortex-induced oscillation, and acoustoelastic vibration.

The papers presented in this volume are quite comprehensive and contain the results of a great deal of recent work. They should provide a good source for researchers as well as practicing engineers. The editors wish to express their thanks to the authors for their willingness to share their experience and expertise and to the reviewers for their conscientious contribution. The editors also wish to thank the Technical Program chairman, Fr. Jeffrey Fong, and the session coordinator, Mr. Greg Hollinger, for their help in organizing the symposium.

S. S. Chen

J. C. Simonis

Y. S. Shin

CONTENTS

FLUID FORCES ON TWO CIRCULAR CYLINDERS IN CROSSFLOW

J. A. Jendrzejczk and S. S. Chen
Components Technology Division
Argonne National Laboratory
Argonne, Illinois

ABSTRACT

Fluid excitation forces are measured in a water loop for two circular cylinders arranged in tandem and normal to flow. The Strouhal number and fluctuating drag and lift coefficients for both cylinders are presented for various spacings and incoming flow conditions. The results show the effects of Reynolds number, pitch ratio, and upstream turbulence on the fluid excitation forces.

1. INTRODUCTION

Multiple circular cylinders are employed in nuclear reactor system components. Examples range from fuel bundles to steam generator tube banks. As in the case of an isolated cylinder, each cylinder is subjected to steady fluid forces and unsteady fluid forces. It is important to understand the interaction of multiple cylinders in flow to avoid detrimental vibration. Two circular cylinders represents the simplest case which possesses the general characteristics of an array of cylinders.

Consider two cylinders (1 and 2; see Fig. 1) subjected to crossflow. Fluid-force components acting on the two cylinders are g_1 and g_2 in the drag direction and h_1 and h_2 in the lift direction. If the cylinders are rigid, these fluid-force components can be written

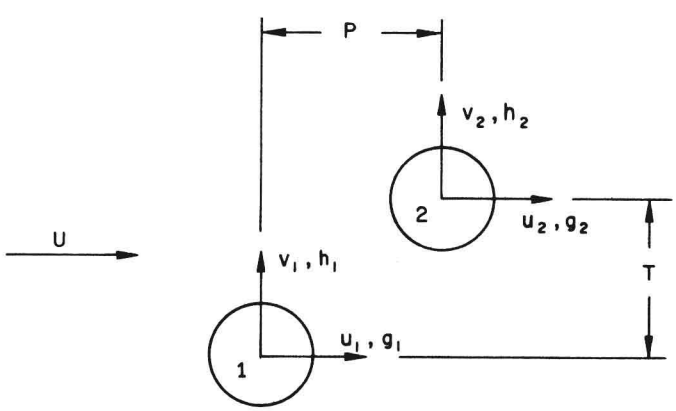

Fig. 1 Two circular cylinders in crossflow

$$g_j = \frac{1}{2}\rho U^2 D C_{Dj} + \frac{1}{2}\rho U^2 D C'_{Dj}\sin(\Omega_{Dj} + \phi_{Dj}) + g'_j \ ,$$

and (1)

$$h_j = \frac{1}{2}\rho U^2 D C_{Lj} + \frac{1}{2}\rho U^2 D C'_{Lj}\sin(\Omega_{Lj} + \phi_{Lj}) + h'_j \ ,$$

$$j = 1, 2 \ ,$$

where ρ is fluid density, U is flow velocity, D is cylinder diameter, C_{Dj} (C_{Lj}) is the steady drag (lift) coefficient of cylinder j (j = 1, 2), C'_{Dj} (C'_{Lj}) is the sinusoidal drag (lift) fluid coefficient, and g'_j and h'_j are fluid forces due to turbulence buffeting.

The fluid-force components given in Eq. 1 are fluid excitation forces. If the cylinders are movable, additional fluid-force components will result from cylinder oscillations. These are the motion-dependent fluid forces, which are given as follows:

$$g_j = \sum_{k=1}^{2} \left(\bar{\alpha}_{jk}\frac{\partial^2 u_k}{\partial t^2} + \bar{\sigma}_{jk}\frac{\partial^2 u_k}{\partial t^2} + \bar{\alpha}'_{jk}\frac{\partial u_k}{\partial t} + \bar{\sigma}'_{jk}\frac{\partial v_k}{\partial t} + \bar{\alpha}''_{jk}u_k + \bar{\sigma}''_{jk}v_k\right)$$

and (2)

$$h_j = \sum_{k=1}^{2} \left(\bar{\tau}_{jk}\frac{\partial^2 u_k}{\partial t^2} + \bar{\beta}_{jk}\frac{\partial^2 u_k}{\partial t^2} + \bar{\tau}'_{jk}\frac{\partial u_k}{\partial t} + \bar{\beta}'_{jk}\frac{\partial v_k}{\partial t} + \bar{\tau}''_{jk}u_k + \bar{\beta}''_{jk}v_k\right) \ ,$$

where u_k and v_k (k = 1, 2) are the displacement components in the drag and lift directions of the cylinder

Table 1. Summary of Published Experimental Data for Two Cylinders in Crossflow

Reference	P/D	T/D	Re x 10^{-4}	Turbulence Intensity, %	Fluid	Measurement Technique	Measured Quantities (see Eqs. 3 and 4)
Jendrzejczyk and Chen (1982)	1.5 1.75 0 0	0 0 1.5 1.75	2.5 to 5	2.3 7.0 7.7	Water	Force transducer	$\bar{C}_D'$, $\bar{C}_L'$, and St
Arie et al. (1983)	2, 3, 4	0	15.7	0.3	Air	Pressure taps	$\bar{C}_D'$, $\bar{C}_L'$
Savkar (1984)	1.2 to 6.0	0	2 to 20	8.5	Air	Load cells	$\bar{C}_L'$ and St

k, $\bar{\alpha}_{jk}$, $\bar{\sigma}_{jk}$, $\bar{\tau}_{jk}$, and $\bar{\beta}_{jk}$ are added mass matrices, $\bar{\alpha}'_{jk}$, $\bar{\sigma}'_{jk}$, $\bar{\tau}'_{jk}$, and $\bar{\beta}'_{jk}$ are fluid damping matrices, and $\bar{\alpha}''_{jk}$, $\bar{\sigma}''_{jk}$, $\bar{\tau}''_{jk}$, and $\bar{\beta}''_{jk}$ fluid stiffness matrices.

Fluid-force components are needed in the design and assessment of various system components. The purpose of the work reported here is to study the unsteady fluid forces for two rigid cylinders in tandem or side by side for different values of pitch ratios, P/D and T/D.

The flow field around a pair of rigid circular cylinders is very complex and has been studied extensively. The objectives of these studies have been, among other things, to measure the fluid force and/or pressure distribution acting on each cylinder, flow velocity profile, and vortex shedding, and to understand the result of flow patterns. An excellent review was published by Zdravkovich (1977).

In contrast to an isolated circular cylinder, data are very limited on the unsteady fluid forces acting on a pair of cylinders. Table 1 summarizes the published data on the fluctuating fluid forces acting on two cylinders (Jendrzejczyk and Chen 1982, Arie et al. 1983, and Savkar 1984). It is evident that there is an urgent need to obtain additional data on fluctuating fluid forces.

2. EXPERIMENTAL SETUP

The experiment was performed in the Flow Induced Vibration Test Facility (FIVTF). The primary system of the loop is filled with demineralized water and consists of four pumps arranged in parallel, feeding a closed accumulator of 30 m^3 (8000 gal). The flowrates of the four pumps are 0.032, 0.063, 0.16, and 0.25 m^3/s (500, 1000, 2500, 4000 gpm) at 1.0 MPa (150 psig) discharge pressure. The pumps discharge individually through their own control and by-pass valves, flowmeters, and piping to the closed accumulator. Thus, by using a combination of pumps and valves, the flowrate can be controlled from ~0.003 m^3/s (50 gpm) to a maximum of 0.5 m^3/s (8000 gpm). From the closed accumulator, water is valved to one of the several test leg branches and returned to a common supply tank of 38 m^3 (10,000 gal).

The test section, shown in Fig. 2, is a square flow channel with a flow area of 30 cm x 30 cm (11-3/4 in. x 11-3/4 in.) connected to one of the test leg branches, which is a 46 cm (18 in.) pipe. A 30 cm (11-3/4 in.) square liner is inserted in the pipe to form a square flow channel upstream and downstream of the test section. The minimum Reynolds number based on the gap flow velocity is ~1.5 x 10^4. With a maximum

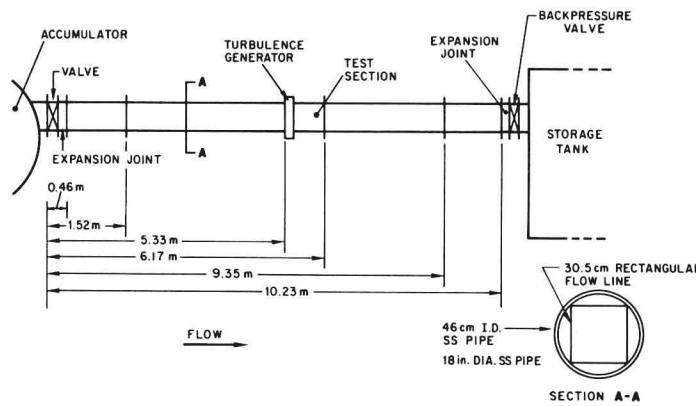

Fig. 2 Test section

flow velocity, a Reynolds number of ~1.5 x 10^5 can be reached. For all measurements, the cylinders with a diameter of 2.54 cm (1 in.) and a length of 29.85 cm (11.75 in.) are used.

Fluid-force components depend on the upstream turbulence. Different grids were placed upstream to vary the flow field. Tests are conducted for three grids: (1) Grid A, (2) Grid B, and (3) Grid C. Grid A is a perforated plate 0.159 cm (0.0625 in.) thick with 0.476 cm (0.1875 in.) diameter holes. Grids B and C were constructed by drilling holes uniformly in a closely-packed array through 2.86 cm (1-1/8 in.) thick plates. The grid and turbulence characteristics are given in Table 2.

To measure fluctuating fluid forces, two piezo-electric three-axial transducers (one at each end of the test cylinder) were used (Fig. 3). The diameter of the test cylinders is 2.54 cm (1 in.) and the active length is the channel width 30 cm (11-3/4 in.). The locations of the test cylinders in the test section for various tests are described in Table 3. Position 5 was an oversize penetration and was not used for force measurements.

3. TEST PROCEDURES AND DATA ANALYSES

A series of single and twin tubes were tested under three turbulence intensities: (1) A single tube, (2) two tubes normal to flow with T/D = 1.35 and 2.7; and (3) two tubes in tandem with P/D = 1.35, 2.7, 4.05, 5.4, 6.75, 8.1, and 10.8.

Table 2. Grid and Turbulence Characteristics*

Grid	X_m, cm	TI, %	L, cm	a, cm	b, %
A	42.3	1-3	4-8.5	0.476	49
B	42.3	4-5	1.2-1.4	1.74	58
C	42.3	10-11	2.3-2.7	2.67	75

*From Mulcahy (1984).

X_m is the distance between downstream surface of the grid and the centerline of the center tube of the test section,
a is the hole diameter,
b is the blockage ratio,
TI is the turbulence intensity, and
L is the length scale.

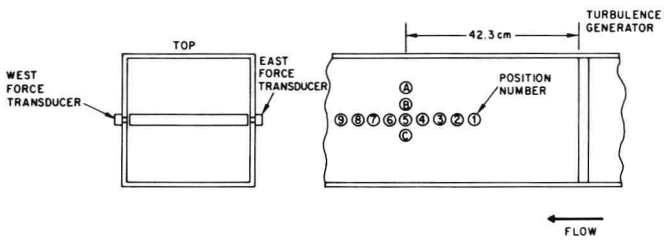

Fig. 3 Cylinders installed in the test section

Table 3. Tube Locations

Arrangement	T/D*	P/D*	Position Tube 1	Position Tube 2
Single tube	--	--	A	B
Two tubes normal	1.35	-	A	B
	2.7	-	B	C
Two tubes In tandem	-	1.35	1	2
	-	2.7	1	3
	-	4.05	1	4
	-	5.4	2	6
	-	6.75	1	6
	-	8.1	1	7
	-	10.8	1	9

*T/D is transverse pitch; P/D is longitudinal pitch.

In each test, fluid pressure, flow velocity, and fluid forces acting on the tubes are measured. The total flowrate is measured by turbine flowmeters. The mean flow velocity is obtained by dividing the flowrate by the flow area. All calculations are based on the gap flow velocity.

In each test run, the flow velocity is increased at small intervals. At each flow velocity, the fluid force components in the lift and drag directions are recorded on a magnetic tape for several minutes for subsequent analysis. A fast Fourier transform analyzer is used to determine fluid force characteristics. Low-pass filters are used to filter out the transducer tube resonant frequency (f_R > 120 Hz).

Fluid excitation forces acting on the tubes are given in Eq. 1. In presentation of the data, RMS fluctuating drag and lift coefficients are given:

$$\bar{C}'_{Dj} = \langle C'_{Dj}\sin(\Omega_{Dj} + \phi_{Dj}) + \frac{2}{\rho U^2 D} g'_j \rangle^{1/2}$$

and (3)

$$\bar{C}'_{Lj} = \langle C'_{Lj}\sin(\Omega_{Lj} + \phi_{Lj}) + \frac{2}{\rho U^2 D} h'_j \rangle^{1/2} ,$$

where < > denotes mean square value of the argument.

The Strouhal number is evaluated from the frequency spectra of fluid force components in the lift direction:

$$St = \frac{fD}{U} , \quad (4)$$

where f is the frequency peaks.

4. EXPERIMENTAL RESULTS

The measurements were taken from subcritical to transition regions $1.5 \times 10^4 < Re < 1.5 \times 10^5$. The gap flow velocity is ~0.6 m/s (1.97 ft/sec) < U_g < 8 m/s (26.2 ft/sec). The results are presented based on the gap flow velocity.

4.1 AN ISOLATED CYLINDER

In Fig. 4, the Strouhal number (St) and rms values of fluctuating lift and drag coefficients ($\bar{C}'_L$ and $\bar{C}'_D$) are plotted against Reynolds number Re. In general, the results match the measurements by So and Savkar (1981), Schewe (1983), Cheung and Melbourne (1983), and Mulcahy (1984).

The Strouhal numbers were obtained from the power spectra of the lift fluctuations. At low flow velocities, typical spectra are narrow-band, with a sharp peak at the Strouhal frequency. At higher flow velocities, the spectra become broad-band with no frequency peaks.

The fluctuating lift and drag coefficients given in Fig. 4 appear to be lower than those by some other measurements (So and Savkar, 1981). This is attributed to the relatively large length-to-diameter ratio of the tube. Since the correlation length of vortex shedding for a single rigid cylinder is ~0.5 D to 6D (King, 1977), the span length of the cylinder of about 12D in this case results in smaller fluctuating fluid-force coefficients.

The decrease in fluctuating lift and drag in the critical flow regime is shown to occur at lower

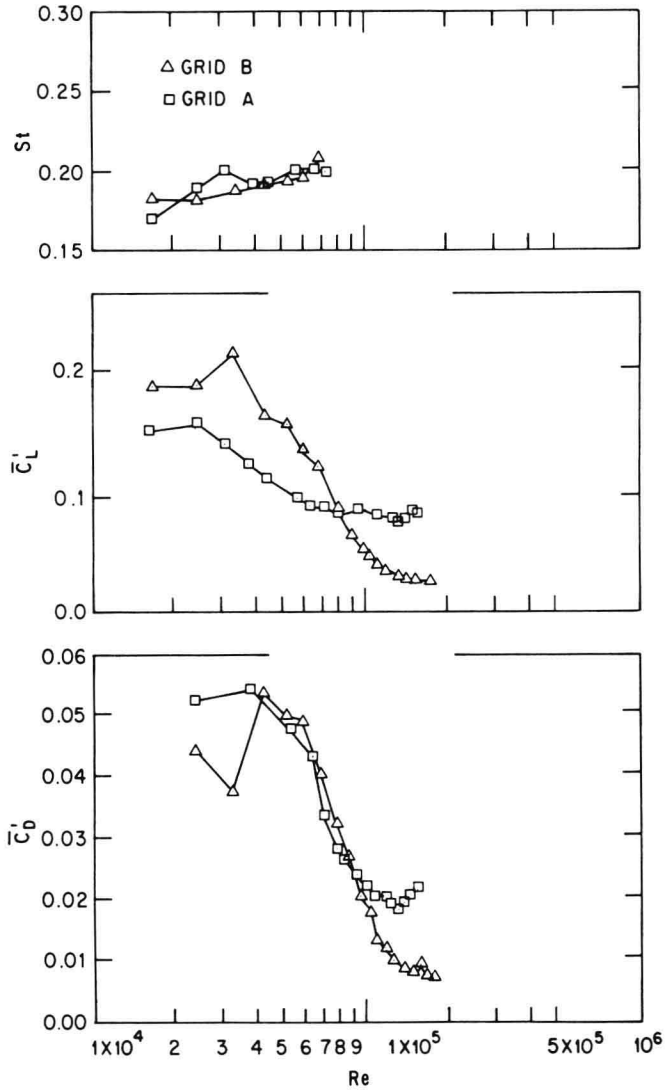

Fig. 4 Strouhal number, and RMS lift coefficients for an isolated cylinder

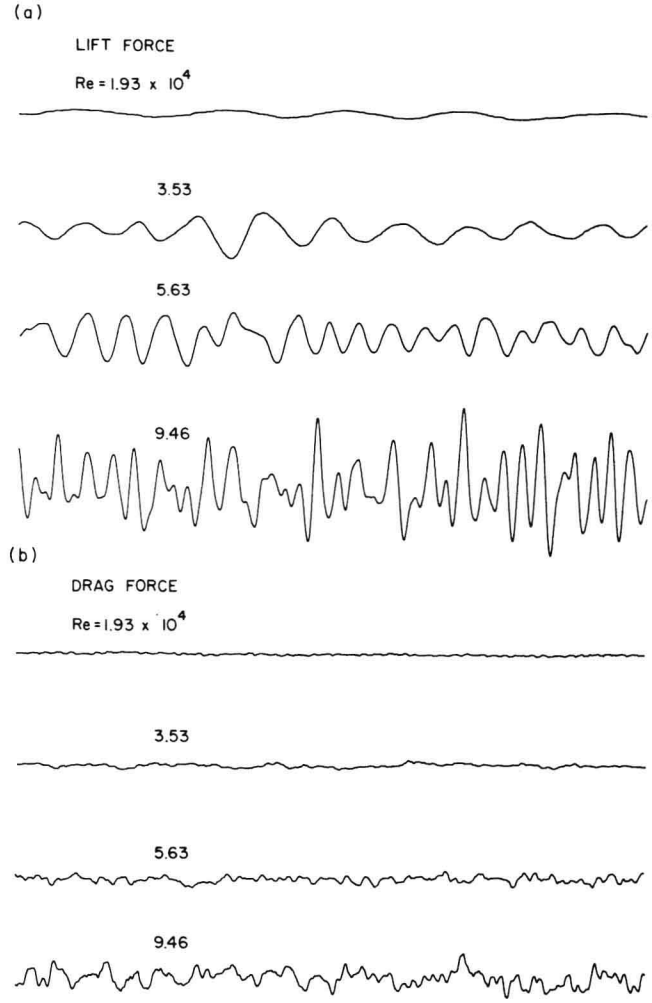

Fig. 5 Fluctuating lift and drag forces on one of the cylinders for two cylinders normal to flow with T/D = 2.7

Reynolds numbers for larger turbulence. This is consistent with other reuslts, e.g., the data by Cheung and Melbourne (1983).

4.2 TWO TUBES NORMAL TO FLOW

The fluctuating lift and drag forces depend on tube pitch, Reynolds number, and incoming flow conditions. Figure 5 shows the fluctuating lift and drag forces for T/D = 2.7 with Grid C and for four representative Re to illustrate the changing nature of the force. At Re = 1.93×10^4, the fluctuating lift is periodic and the drag force is very small. With the increase of Re, the lift force changes from highly organized to more random. The organized nature of the lift force is indicative of the orderly alternate vortex shedding. At higher Re, the shed vortices would no longer have a distinct frequency. These characteristics are basically the same as those for an isolated cylinder.

The characteristics of the fluctuating lift and drag can also be noted from the frequency spectra given in Fig. 6. At low Re, there is only one distinct peak in the spectra and the vortex shedding frequencies can be determined without ambiguity. As Re is increased, the frequency peak becomes less distinct, resulting in no identifiable peak at high Re.

Figure 7 shows the Strouhal number for two cylinders normal to flow. For T/D = 2.7, the Strouhal number is the same as that for a single cylinder. For T/D = 1.35, in some range of Re, two vortex frequencies are noted. This agrees with previous investigations (Zdravkovich 1977, Arie et al. 1983, and Bearman and Wadcock 1973).

Figure 8 shows the rms values of fluctuating lift and drag as a function of Re for T/D = 1.35 with Grid B.

For two cylinders normal to flow with $1.2 < T/D < 2.0$, the gap flow is biased to one side (Bearman and Wadcock, 1973). Consequently, wide and narrow wakes are formed behind the cylinders. Apparently, the biased flow pattern does not affect the fluctuating drag and lift; these force components measured from the two cylinders are about the same for both T/D = 1.35 and 2.7.

The general trend of the variation of drag with Re is similar to that of lift. In the subcritical region, the drag coefficient is ~20-25% of the lift coefficient. In the transition region, $\bar{C}_D'/\bar{C}_L'$ may be as large as 0.5.

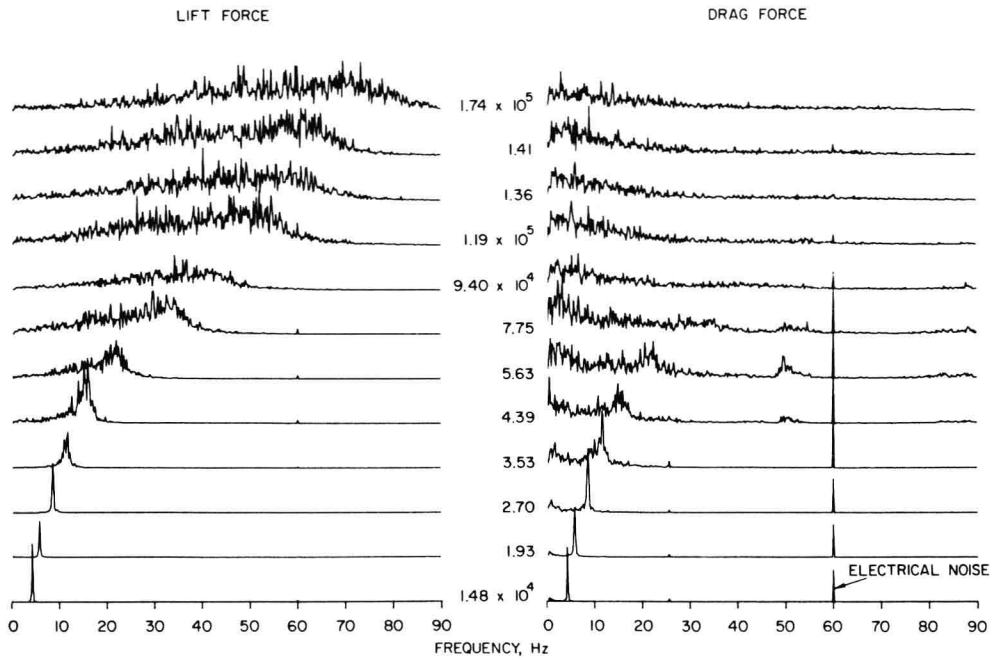

Fig. 6 Frequency spectra of the lift and drat forces for two cylinders normal to flow for T/D = 2.7 with Grid C

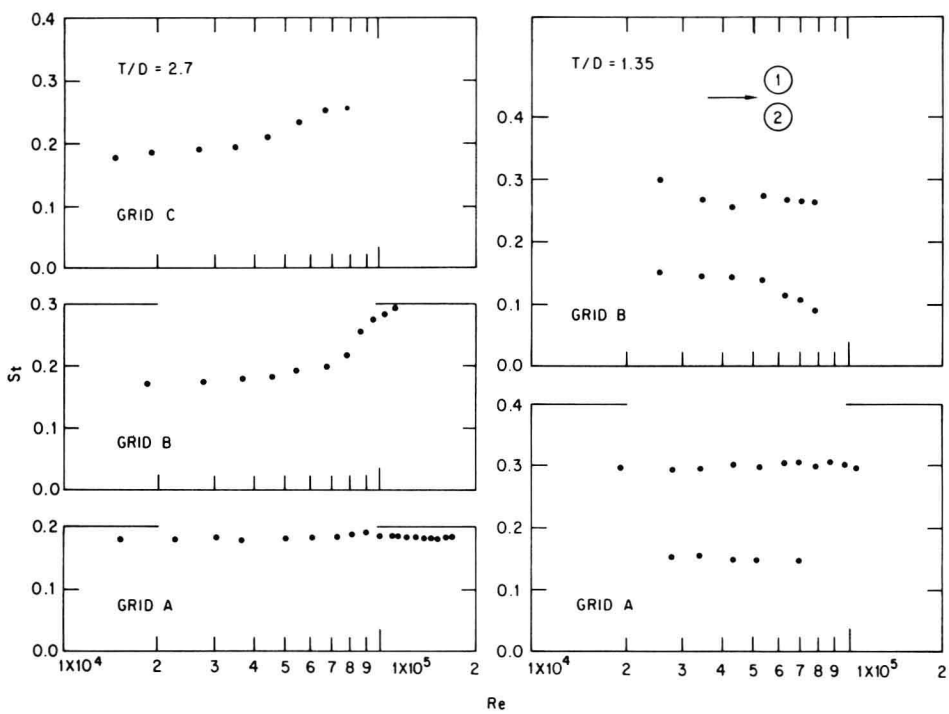

Fig. 7 Strouhal numbers for two cylinders normal to flow

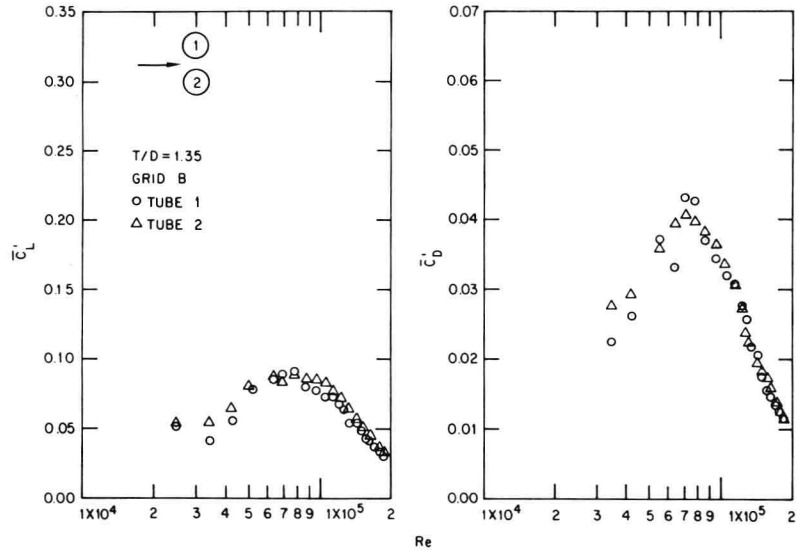

Fig. 8 Fluctuating drag and lift coefficients for T/D = 1.35 and Grid G

The pitch ratio plays an important role. In the subcritical Re, $\bar{C}_L'$ and $\bar{C}_D'$ are larger for T/D = 2.70. However, in the transition region, both $\bar{C}_L'$ and $\bar{C}_D'$ are approximately the same for T/D = 2.7 and 1.35. In addition, the transition region for T/D = 2.7 occurs at lower Re.

The effect of the upstream turbulence is similar to that of an isolated cylinder; it reduces the effective Re for the transition region.

4.3 TWO TUBES IN TANDEM

The time histories of the lift forces for two tubes in tandem are similar to those of two tubes normal to flow. At Re = 3.45×10^4, both lift forces exhibit very orderly oscillations. At higher Re, the lift force on tube 2 (downstream tube) is more orderly than on tube 1.

Typical frequency spectra of the lift and drag forces for two tubes in tandem are given in Figs. 9 and 10.

Figure 9 shows the frequency spectra of lift force for two tubes in tandem with P/D = 1.35 and Grid A. The frequency peak for Tube 2 is the usual Strouhal frequency, with St varying from 0.14 to 0.16 for Re from 10^4 to 1.5×10^5. For Tube 1, in addition to the Strouhal frequency, there is another frequency peak with its frequency equal to approximately one third of the Strouhal frequency. At higher Re, the response associated with the higher frequency decreases with flow, while that associated with the lower frequency peak becomes dominant. The cause of the lower frequency peak is unknown.

The frequency spectra change from those with a sharp peak to a broad-band spectrum at high Re. This is similar to those of an isolated tube in crossflow and other published results. However, in the literature, it is reported that no vortex shedding is detected behind the front tube (Zdravkovich, 1977); the results of these tests show clearly that there is a resultant fluctuating lift force on the front tube.

Figure 10 shows the frequency spectra of drag and lift for Tube 2 for P/D = 2.7 and Grid A. The Strouhal frequency in the lift direction is easily recognized. In the drag direction, there is a frequency peak occurring at twice the Strouhal frequency. This, too, is similar to that of an isolated tube.

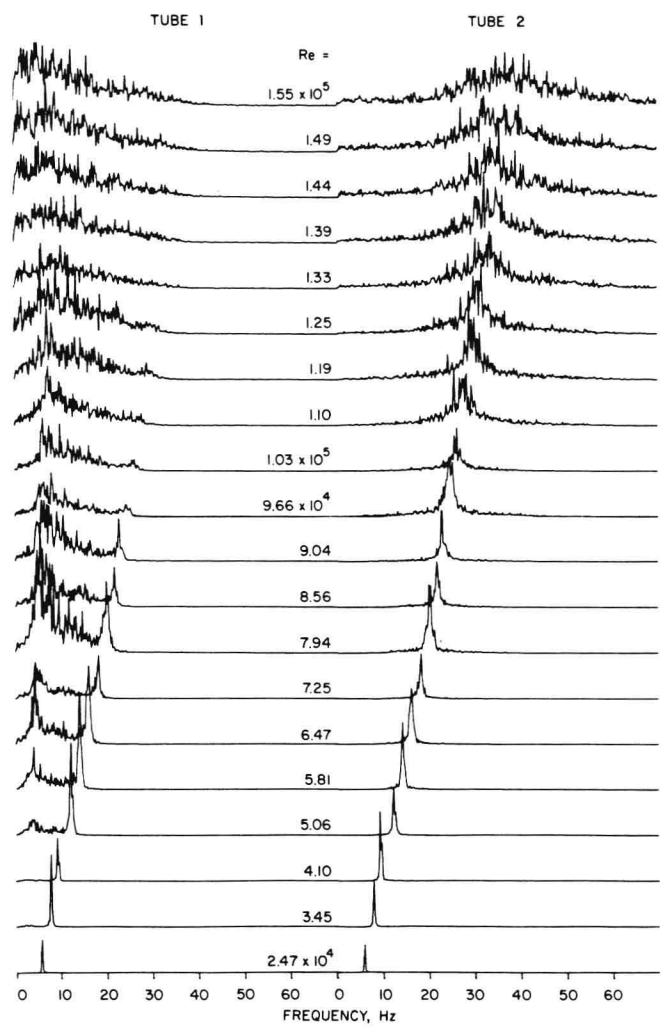

Fig. 9 Frequency spectra of the lift forces for two cylinders in tandem for P/D = 1.35 and Grid A

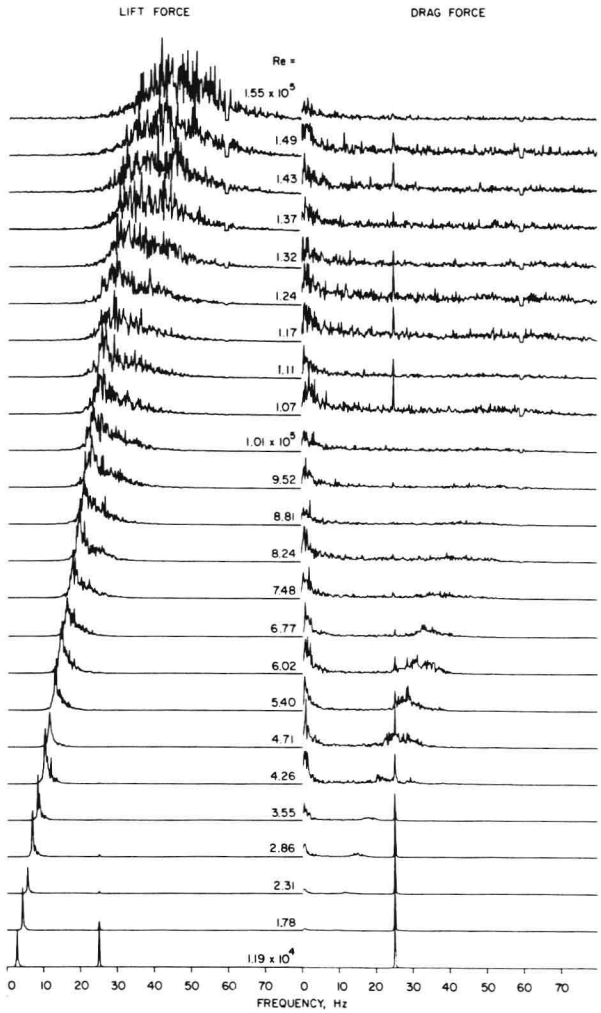

Fig. 10 Frequency spectra of the lift and drag forces acting on the downstream cylinder for two cylinders in tandem for P/D = 2.7 and Grid A

Based on the frequency spectra, the general characteristics of the lift and drag for different cases are summarized in Table 4. The characteristics fall into three categories:

(1) The frequency spectra of the lift or drag force do not exhibit dominant frequency peaks.

(2) At low Re, there is a frequency peak associated with the vortex shedding and at high Re, there are no dominant frequency peaks in the spectra.

(3) At low Re, there are two frequency peaks, one at the Strouhal frequency and the other at twice the Strouhal frequency. At high Re, there are no dominant frequency peaks.

Based on the frequency spectra, some general conclusions are noted on the Strouhal frequency:

- C'_{L1} - Except at P/D = 1.35 with Grid C, there exists a Strouhal frequency at subcritical Re.
- C'_{D1} - Except at large P/D (6.75 to 10.8) with low turbulence, there are no frequency peaks.
- C'_{L2} - Except at P/D = 1.35 with Grid C, there exists a Strouhal frequency at subcritical Re.
- C'_{D2} - At large P/D ($\geq$ 5.4), there are frequency peaks at the Strouhal frequency and twice the Strouhal frequency.

The Strouhal numbers are given in Fig. 11 for both tubes. Tube 2 is a greater distance from the turbulence grid; therefore, it experiences less turbulence from the incoming flow. The Strouhal frequency at higher flow velocity for Tube 2 is much more well defined.

Figure 12 compares St among this study and the data by Bokaian and Geoola (1984) and Kiya et al. (1980) at the subcritical Re. Both Bokaian and Geoola and Kiya et al. used a hot-wire anemometer placed in the wake of the cylinder to measure the velocity fluctuation. The results from three tests agree reasonably well. The vortex shedding behind the upstream tube is suppressed up to P/D = 3. Kiya et al. noted weak spectrum peaks in the velocity fluctuation induced behind the upstream tube by the periodic vortex shedding from the downstream tube. The results of this study show clear frequency peaks for P/D = 1.35 and 2.7. This suggests that even though no distinct vortices were found behind the upstream tube, the fluctuating lift of the upstream cylinder does not depend on the distinct vortices.

For two tubes in tandem, the critical spacing (P/D) is approximately between 3.0 and 3.8. For P/D < 3.0, Kiya et al. found no distinct vortex shedding behind the upstream tube, and St for the downstream tube increases with decreasing P/D. For P/D > 3.8, St behind the upstream tube increases with P/D for up to about 6 ~ 7 and then approaches to that of an isolated tube at P/D ~ 10. St for the downstream tube obtained by Kiya et al. shows a jump at P/D = 3 to 3.8; however, St obtained by Bokaian and Geoola shows no discontinuity.

The Strouhal number for two tubes in tandem can be used to evaluate the Strouhal number for a single cylinder. When P/D is large, the Strouhal number for the upstream cylinder is the same as that for a single tube. Based on the results presented in this paper, the Strouhal number in the transition region can be sketched as shown in Fig. 13. The values of St depend on the upstream TI; the higher the TI, the smaller the St. This is one of the reasons that there is a great scattering in this region.

RMS values of fluctuating lift and drag forces for grid A are given in Figs. 14 through 17. Some general characteristics are noted.

- $\overline{C}'_{L1}$ and $\overline{C}'_{D1}$ are dependent on the pitch ratio for P/D < 4.05. For P/D > 4.05, $\overline{C}'_{L1}$ and $\overline{C}'_{D1}$ are not affected appreciably by P/D.
- $\overline{C}'_{L2}$ is dependent on P/D for 1.35 and 2.7. For P/D = 4.05 to 10.8, there are variations.
- $\overline{C}'_{D2}$ varies significantly with P/D for 1.35, 2.7 and 4.05, and for P/D > 5.4, there is little change.

The rms lift and drag coefficients are functions of Reynolds number, pitch ratio, and turbulence. Figure 18 shows the rms C'_L and C'_D as a function of P/D for Re = 10^5. In general, the rms lift and drag for the downstream cylinder are larger than the upstream one for smaller spacing. However, at high turbulence and very small P/D, the upstream will experience larger C'_L because of the incoming flow. For larger P/D, they approach those of an isolated cylinder. Similar results are obtained by Arie et al. (1983) for subcritical Re.

Figure 19 shows the fluctuating lift with P/D = 4.05 and 10.8 and Grids B and C. The effects of turbulent intensity are to shift the transition region to a low Re range. Similar characteristics are noted for the downstream tube. In addition, the fluctuating force components are reduced with increasing turbulence in the subcritical Re.

Table 4. Frequency Spectra Characteristics for Two Cylinders in Tandem

Grid	Tube No.	Force Component	P/D 1.35	2.7	4.05	5.4	6.75	8.1	10.8
A	1	Drag	x	x	x	x	o	o	o
		Lift	●	●	●	●	●	●	●
	2	Drag	x	x	x	o	o	o	o
		Lift	●	●	●	●	●	●	●
B	1	Drag	x	x	x	x	x	x	o
		Lift	●	●	●	●	●	●	●
	2	Drag	x	x	x	o	o	o	o
		Lift	●	●	●	●	●	●	●
C	1	Drag	x	x	x	x	x	x	x
		Lift	x	●	●	●	●	●	●
	2	Drag	x	x	x	x	o	o	o
		Lift	x	●	●	●	●	●	●

x No dominant frequency peaks.

● One frequency peak associated with the vortex shedding at low Re and no dominant frequency peaks at high Re.

o Two frequency peaks, one at the Strouhal frequency and the other at twice the Strouhal frequency at low Re, and no dominant frequency peaks at high Re.

5. CONCLUDING REMARKS

This report describes the fluctuating drag and lift forces acting on a pair of cylinders side by side or in tandem. The fluid forces are measured at a Reynolds number from about 1.5×10^4 to 1.5×10^5 for several turbulence intensities in the incoming flow.

Two cylinders in crossflow have application to nuclear reactor system components as well as having many other engineering applications. The characterization of the fluid forces is an integrated part of understanding the dynamic response of such a system. Extensive measurements have been reported on steady-state fluid-force components; however, very limited information is available for fluctuating fluid-force components, in particular, at high Reynolds numbers. The information presented in this report provides some of this necessary data for two tubes in crossflow.

A complete characterization of a two-tube system in crossflow requires not only fluid excitation force components, as presented in this report, but motion-dependent fluid forces, as well. Measurements of motion-dependent fluid force will require measurements of fluid forces acting on moving cylinders.

The study of a single cylinder in crossflow has a history of more than a hundred years; however, a complete analysis in terms of the fundamental principles of fluid mechanics remains under development, and some of the features of the vibration of a single cylinder in crossflow remain not well understood. For two cylinders, there are infinite numbers of arrangements; therefore, since it is much more complicated, it is that much more difficult to provide a complete description of the two-tube system. It is expected that research in this problem will continue steadily.

ACKNOWLEDGMENTS

Work supported by the U.S. Department of Energy Assistant Secretary for Nuclear Energy, Office of Reactor Systems, Development, and Technology, under contract No. W-31-109-Eng-38.

G00355